индекс 3624

ԵՐԵՎԱՆԻ ՖԻԶԻԿԱՅԻ ԻՆՍՏԻՏՈՒՏ
ЕРЕВАНСКИЙ ФИЗИЧЕСКИЙ ИНСТИТУТ

ЕФИ-581(68)-82

A.S.BAGDASARYAN, S.V.ESAYBEGYAN, N.L.TER-ISAAKYAN

RELATIVISTIC QUARK MODEL AND BEHAVIOR OF THE MESON ELECTROMAGNETIC FORM-FACTORS AT SMALL AND INTERMEDIATE MOMENTUM TRANSFER Q^2

ԵՐԵՎԱՆ 1982 ЕРЕВАН

ЕФИ-581(68)-82

А.С.БАГДАСАРЯН, С.В.ЕСАЙБЕКЯН, Н.Л.ТЕР-ИСААКЯН

РЕЛЯТИВИСТСКАЯ МОДЕЛЬ КВАРКОВ И ПОВЕДЕНИЕ ЭЛЕКТРОМАГНИТНЫХ ФОРМФАКТОРОВ МЕЗОНОВ В ОБЛАСТИ МАЛЫХ И ПРОМЕЖУТОЧНЫХ Q^2

В модели адронов, состоящих из релятивистских кварков, получено согласованное с экспериментальными результатами описание статических характеристик мезонов и электромагнитного формфактора пиона в области малых и промежуточных значений $0 \le Q^2 \le 6 (ГэВ/с)^2$

Ереванский физический институт
Ереван 1982

YEREVAN PHYSICS INSTITUTE

ЕФИ-581(68)-82

A.S.BAGDASARYAN, S.V.ESAYBEGYAN, N.L.TER-ISAAKYAN

RELATIVISTIC QUARK MODEL AND BEHAVIOR OF THE MESON ELECTROMAGNETIC FORM-FACTORS AT SMALL AND INTERMEDIATE MOMENTUM TRANSFER Q^2

Yerevan 1982

1. Introduction

The investigation of the hadron electromagnetic form factors at large momentum transfer gives significant information on the inner dynamics of hadrons and the structure of hadronic wave functions.

The concept of hadron as a composite system of a finite number of quarks leads to quark counting rules [1,2] which give for the form factors

$$F(Q^2) \sim 1/Q^{2(n-1)} \qquad (1)$$

where n is the number of quarks in a hadron. In the perturbative QCD the power law (1) corresponds to one-gluon exchanges between the quarks composing a hadron (fig. 1). The data available on nucleon and meson form factors agree with the power behavior (1) which was treated as an experimental confirmation of the one-gluon exchange model. In subsequent papers, within the framework of the perturbative QCD exact theoretical predictions were obtained for the asymptotic behavior of form factors taking into account logarithmic corrections to the po-

wer law (1). These results proved to be in a deep discrepancy with the experimental data. For instance, the experimental value of the pion form factor at $Q^2 \sim 6(\text{GeV/c})^2$ exceeds the theoretical prediction 5-6 times (see e.g. [3]). The neutron magnetic form factor is predicted positive at $Q^2 \to \infty$, and that of proton should be asymptotically suppressed as compared with the neutronic [4,5]. It should be emphasized that the magnitudes of form factors at large q^2 essentially depend on the hadronic wave functions. The above discrepancy with the experiment takes place for the asymptotic at $Q^2 \to \infty$ wave functions which have been obtained in the perturbative QCD by an evolution equation solution or operator product expansion method (see e.g. [3,5,6]). In a number of papers [3,7] it was assumed that at available values of Q^2 the wave function essentially differs from the asymptotic one, and an attempt was made to construct a low-energy pion wave function [7] to bring theoretical values of the form factor to an agreement with the experiment. Difficulties associated with the one-gluon exchange model in the description of an electromagnetic form factor stimulated a number of papers, where the form factor behavior was investigated on the basis of a different physical picture. In ref. [8], within the framework of topological expansion and the colored tube model a good description of the proton magnetic form factor at $Q^2 > 2 \div 3(\text{GeV/c})^2$ was obtained. In refs. [9,10,11] a good description of the pion form factor at $0.5 < Q^2 < 5(\text{GeV/c})^2$ was obtained using the QCD dispersion sum rules.

In this paper the possibility of a combined description

of meson low-energy characteristics and pion electromagnetic form factor in the range of small and intermediate values of Q^2 in the relativistic quark model [12-14] is investigated. Low-energy wave functions of π and ρ -mesons which give a good description of f_π ($\pi \to \mu\nu$ decay constant), f_ρ ($\rho \to \gamma$ transition constant), $g_{\omega\pi}$ ($\omega \to \pi\gamma$ decay amplitude) and R_π^2 (pion mean-square radius), are constructed phenomenologically. It is shown that in such a model the data available on $F_\pi(Q^2)$ may be described basing on a simplest quark diagram without gluon exchanges (fig. 2). The contribution of a one-gluon exchange diagram in such a model cannot exceed 30%.

2. Low-Energy Characteristics of Mesons

Let us now turn to the consideration of the static characteristics of mesons. The quantities f_π, f_ρ, $g_{\omega\pi}$ and $\langle R_\pi^2 \rangle$ were first calculated in the framework of a relativistic quark model in the light front dynamics in refs. [12,14].

Later we will use the formulation of relativistic quark model in the infinite momentum frame (IMF) which is based on the consideration of time-ordered diagrams of the old fashioned perturbation theory. Such a formulation of the model is presented in detail in ref. [15], where, in particular, is given a general method of constructing vertex functions of a hadron-quark transition corresponding to SU(6)× O(3) classification of hadronic states. The vertex functions for π and $\rho(\omega)$ mesons which are of interest for us, have the following form [15]

$$\Gamma^{\pi}_{s_1 s_2} = \frac{i\delta_{ij}\,\psi_{\pi}(P_1,P_2)}{\sqrt{6}\,2M_0^2(M_0+2m)}\,\bar{u}^i_u(P_1)(\hat{P}_0+M_0)\gamma_5(-\hat{P}_0+M_0)v^j_{\bar{d}}(-P_2) \quad (2)$$

$$\Gamma^{\rho}_{s_1 s_2;s} = \frac{\delta_{ij}\,\psi_{\rho}(P_1,P_2)}{\sqrt{6}\,2M_0^2(M_0+2m)}\,\bar{u}^i_u(P_1)(\hat{P}_0+M_0)\gamma_\mu(-\hat{P}_0+M_0)v^j_{\bar{d}}(-P_2)\ell^s_\mu(P_0) \quad (3)$$

where P_1 and P_2 are the momenta of u and $\bar{d}$ quarks; $P_0=P_1+P_2$, m is the mass of u and $\bar{d}$ quarks; $M_0^2=P_0^2$ is the invariant mass of the system of quarks composing a meson; $\ell^s_\mu(P_0)$ is the ρ-meson polarization vector; i, j are color indices. Radial parts of the vertex functions $\psi_\pi(P_1,P_2)$ and $\psi_\rho(P_1,P_2)$ describe the momentum distribution of quarks in mesons.

Vertex functions (2)-(3), written in the rest frame $\vec{P}_0=0$ via Pauli spinors, have a standard SU(6) structure.

Let's introduce Feynman parametrization in the infinite momentum frame $\vec{P}_0\to\infty$:

$$\vec{P}_i = x_i\vec{P}_0+\vec{K}_{i\perp};\quad \sum_{i=1}^{2}\vec{K}_{i\perp}=0;\quad \sum_{i=1}^{2}x_i=1 \quad (4)$$

The parameter x_i may be related to quark momenta in the rest frame $\vec{P}_0=0$ $\quad K_i=(\omega_i,\vec{K}_i)$

$$x_i=\frac{\omega_i+(K_i)_z}{2\omega_i};\quad \omega_i=\sqrt{K_i^2+m^2} \quad (5)$$

Vertex functions (2-3) in the frame $\vec{P}_0\to\infty$ have a standard SU(6) structure if expressed via two-component spinors:

$$W_s=\sum_{s'}W_{s'}\,U_{s's}(\bar{K}_i) \quad (6)$$

where the matrix

$$U(\bar{K}_i)=\frac{m+\omega_i+(K_i)_z+i\epsilon_{mn}\sigma_m\vec{K}^{\perp}_{in}}{\sqrt{\bar{K}^2_{i\perp}+(m+\omega_i+(K_i)_z)^2}} \quad (7)$$

coincides with the Melosh matrix [16].

Considering corresponding quark diagrams of old fashioned perturbation theory in IMF (fig. 2) and making use of the vertex functions (2,3), one may easily obtain the following expressions for the quantities f_π, f_ρ, $f_{\omega\pi}$ and for the contribution of the fig. 2 diagram to the pion electromagnetic form factor denoted by $F^{\pi}_{(0)}(q^2)$:

$$f_\pi=\sqrt{2}\int_0^1\varphi_\pi(x)\,dx \quad (8)$$

$$f_\rho=\sqrt{2}\int_0^1\varphi_\rho(x)\,dx \quad (9)$$

$$f_{\omega\pi}=\frac{\sqrt{4\pi\alpha}}{32\pi^2}\int_0^1\left\{\frac{2m\omega}{K_\perp^2+m^2}+\frac{K_\perp^2\omega}{(\omega+m)(K_\perp^2+m^2)}\right\}\frac{\omega\,dK_\perp^2dx}{x(1-x)}\phi_\pi(K_\perp^2,x)\phi_\omega(K_\perp^2,x) \quad (10)$$

$$F^{\pi}_0(q^2)=\frac{1}{64\pi^2}\int_0^1\frac{dx}{x^2(1-x)^2}\int_0^\infty dK_\perp^2\left(m^2+K_\perp^2-\frac{(1-x)^2q_\perp^2}{4}\right)\cdot$$
$$\cdot\,\phi_\pi\left[\left(K_\perp-\frac{(1-x)q_\perp}{2}\right)^2,x\right]\phi_\pi\left[\left(K_\perp+\frac{(1-x)q_\perp}{2}\right)^2,x\right] \quad (11)$$

Note that when calculating the diagrams of figs. 2a and 2b one should use IMF where $q_0\sim q_3\sim q_\perp^2/4p$. In (10-11) $\omega=\sqrt{K^2+m^2}$; vertex functions $\Phi(K_\perp^2,x)=\Psi(P_1,P_2)\sqrt{M^2-M_0^2}$ differ from corresponding functions of ref. [14] by a factor $\sqrt{4\pi\alpha}$. The normalization condition of vertex functions $\Phi(K_\perp x)$ may be obtained from $F^{\pi}_{(0)}(P)=1$

$$\frac{1}{64\pi^2}\int_0^1 \frac{dx}{x^2(1-x)^2}\int_0^\infty dK_\perp^2\,(m^2+K_\perp^2)\,|\Phi(K_\perp^2,x)|^2 = 1 \qquad (12)$$

Functions $\varphi_\pi(x)$ and $\varphi_\rho(x)$ are connected with the vertex functions $\Phi_\pi(K_\perp^2,x)$ and $\Phi_\rho(K_\perp^2,x)$:

$$\varphi_\pi(x) = \frac{\sqrt{3}\,m}{16\sqrt{2}\,\pi^2 x(1-x)}\int_0^\infty \Phi_\pi(K_\perp^2,x)\,dK_\perp^2 \,; \qquad (13)$$

$$\varphi_\rho(x) = \frac{\sqrt{3}\,m}{16\sqrt{2}\,\pi^2 x(1-x)}\int_0^\infty \Phi_\rho(K_\perp^2,x)\left(1+\frac{K_\perp^2}{m(\omega+m)}\right)dK_\perp^2 \qquad (14)$$

The width of $\omega\to\pi\gamma$ decay is connected with the amplitude $f_{\omega\pi}$ as follows:

$$\Gamma_{\omega\pi} = \frac{f_{\omega\pi}^2}{12\pi}\left[\frac{m_\omega^2 - m_\pi^2}{2m_\omega}\right]^3$$

The formulae (10-11) are obtained without consideration of anomalous magnetic moments (a.m.m.) of quarks. In fact, as is seen from the detailed analysis of the nucleon low-energy characteristics [17], constituent quarks do posses a.m.m.

$$\mathcal{K}_i^{a.m} = \mathcal{K} Q_i + \tilde{\mathcal{K}} \qquad (15)$$

where

$$\mathcal{K} = 0.071 \pm 0.04 \qquad (16)$$

$$\tilde{\mathcal{K}} = -0.035 \pm 0.015 \qquad (17)$$

Introducing a.m.m. not proportional to the quark charge $\tilde{\mathcal{K}} \sim -0.035$, one may describe the ratio of decay widths $\Gamma(\omega\to\pi\gamma)/\Gamma(\rho\to\pi\gamma)$ [17], therefore, in a later numerical analysis we will not consider the quantity $\Gamma_{\rho\to\pi\gamma}$ as well as th

constant f_ω connected with f_ρ by the SU(3)-symmetry relation $f_\rho = 3 f_\omega$. Taking into account the quark a.m.m. $\mathcal{K} = 0.071$ leads to an approximately 10% increase of the values $\langle R_\pi^2\rangle$ and $f_{\omega\pi}$.

Formulae (10-11) are equivalent to the corresponding results of ref. [14] and formulae (8-9) differ from them by a factor of $\sqrt{3}$. This is due to the fact that in [14] uncolored quarks were considered.

When carrying out the numerical analysis we assume that at least in the characteristic range of variables variation the vertex functions $\Phi(K_\perp^2, x)$ may be considered as functions of one variable [14] M_0^2, - invariant mass of a system of quarks composing meson, and for the quantities $\Phi(K_\perp^2, X) = \Phi(M_0^2)$ we have assumed an exponential form

$$\Phi(M_0^2) = \frac{2\pi N}{\Lambda^2}\, e^{-M_0^2/4\Lambda^2} \qquad (18)$$

where N is the normalization parameter. We assumed that $\Phi_\omega = \Phi_\rho$

We analyse the experimental data in the following way. Fixing the quark mass m we find the corresponding values of Λ_π and Λ_ρ by the linear least squares fit. We have obtained a good description of the experimental data in a wide range of parameter values. Theoretical predictions are presented in the Table taking into account a.m.m. of quarks. First and third columns correspond to the boundary values of m beginning from which the experimental data description becomes unsatisfactory. As is seen from the Table, quarks in mesons should be relativistic ($K^2/m^2 = 2\div3$) and the values of quark mass is consistent with the value $m = 0.275 \pm 0.020$ GeV

obtained from the nucleon data analysis. It is interesting that the experimental data allow a good description at $\Phi_\rho(M_o^2) = \Phi_\pi(M_o^2) = \Phi_\omega(M_o^2)$, i.e., the SU(6)-symmetry relations are fulfilled for the vertex functions.

Note that in ref. [14] the consistent description of the meson low-energy parameters was not obtained due to the omitted in (8-9) color factor [3].

3. Pion Electromagnetic Form Factor

The pion electromagnetic form factor in the range of not very large momentum transfer Q^2 should be determined by the sum of fig. 1a and fig. 2a diagrams contribution. The contribution of the simplest diagram without gluon exchanges (fig.2 is presented in the previous section (2). Let's now turn to one-gluon exchange diagrams. Considering energy denominators of the old fashioned perturbation theory in any frame where initial and final mesons move with large momenta, one may show that diagrams of the type shown in figs. 1b,c, violating the space-time picture corresponding to the nonrelativistic quantum mechanics, are suppressed at least as $1/Q^2$, compared with basic diagrams of the type of fig. 1a. The calculations can be most easily carried out in the Breit frame. Turning in the diagrams of the type of fig. 1a, where the vertex functions (2) are used, to two-component spinors and making use of the Melosh matrices (7), we obtain

$$F^{\pi}_{(1)}(Q^2) = \frac{32\pi\alpha_s(Q^2)}{9Q^2}\int_0^1 \frac{\varphi_\pi(x)\,dx}{2x(1-x)}\int_0^1 \frac{\varphi_\pi(y)\,dy}{2y(1-y)} \qquad (19)$$

where functions $\varphi_\pi(x)$ are defined according to (13); $\alpha_s = 4\pi g^2$ is the quark-gluon coupling constant. Eq. (19) is equivalent to corresponding ones of refs. [3,5,6]. The following circumstance should be mentioned. When calculationg the pion form factor (19) the two-quark system form factor (the result of calculating the fig. 1a type diagrams with free initial and final quark lines) is convoluted with the effective wave function.

$$\tilde{\varphi}^{\pi}_{\alpha\beta} = \frac{\sqrt{3}\,m}{16\sqrt{2}\,\pi^2 x(1-x)}\int_0^\infty U_{\alpha\alpha'}(k)\,U_{\beta\beta'}(-k)\,\Phi_\pi(K_\perp^2, x)\,\varphi^{\pi}_{\alpha'\beta'}\,dK_\perp^2 = \varphi^{\pi}_{(x)}\varphi^{\pi}_{\alpha\beta} \qquad (20)$$

where $\varphi_{\alpha\beta} = \frac{1}{\sqrt{2}}(-i\sigma_2)_{\alpha\beta}$ is the SU(6) pion wave function. Thus, wave functions having a standard SU(6)-spin structure are effective in one-gluon exchange duagrams. This is due to the fact that the two-quark system form factor in the main $1/Q^2$ asymptotics is independent of transverse momenta of initial and final quarks, and integrals over $K_\perp$ and $K'_\perp$ are factorized. As a result in the Melosh matrices (7) the linear in $K_\perp$ terms, which could violate the standard spin structure of the pion wave function, give no contributions.

It is natural to identify the function $\varphi_\pi(x)$ with the pion low-energy wave function in the evolution equation [5] and thus estimate the pion effective wave function $\varphi(x, Q^2)$ at arbitrary Q^2. However, in our case there is no need in it, since at our values of the parameters m and Λ^2 the function $\varphi_\pi(x)$ (13) slightly differs from the asymptotic wave function $\varphi(x) = 3\sqrt{2}\,f_\pi\,x(1-x)$ [3]. (see fig. 3). This means that logarithmic corrections are

small and the use of the effective wave function instead of the asymptotic one increases the value of $F_{(1)}(Q^2)$ but slightly.

The contribution of the one-gluon exchange diagram for the case m =0.24 GeV Λ_π =0.442 GeV is presented in fig. 4 (the lower curve). At such values of parameters the wave function behaves in the characteristic range of the variables approximately as $\sqrt{x(1-x)}$. As is seen from the figure, by means of one-gluon exchange diagram one may describe at best 30% of the experimental values of form factor. It should be also noted that the situation isn't improved by the use of exotic wave functions having zeros or dips at $x \sim 0.5$ [7]. For example, one can obtain a satisfactory description of meson static characteristics (finding corresponding values of m and Λ) with the wave function

$$\Phi(k_\perp^2, x) = \frac{120\pi^2 f_\pi}{m\sqrt{3}\,\Lambda^2}[x(1-x)(2x-1)]^2 e^{-k_\perp^2/4\Lambda^2}$$

the integral of which, according to (13), gives a wave function proposed in ref. [7] $\varphi(x) = 15\sqrt{2}\,x(1-x)(2x-1)^2 f_\pi$ but for such a function the contribution of fig. 2a diagram to the pion form factor essentially exceeds its experimental value at $Q^2 > 1(\mathrm{GeV/c})^2$ (the upper curve in fig. 4).

Consider now the contribution of the simplest quark diagram in the pion electromagnetic form factor (fig. 2a). Results for the values of the parameters m = 0.24 GeV, Λ_π =0.442GeV and m =0.28GeV, Λ =0.39GeV are presented in fig.4. As is seen from fig. 4, the formula (11) describes well all

experimental points at $0 \le Q^2 \lesssim 6(\mathrm{GeV/c})^2$. It is interesting that the results in this range weakly depend on the type of the pion wave function (18), and the $F_0(Q^2)$ behaves approximately as $m_0^2/Q^2 + m_0^2$, where the parameter m_0 slowly varies from m_0 = 0.74 GeV at Q^2 = 0 to m_0 =0.61 GeV at Q^2 = 5(GeV/c)^2. (For the case m = 0.24 GeV, Λ_π = 0.442 GeV). The existence of the range of intermediate values of Q^2 , where the power behavior independent of the type of the vertex function is approximately reproduced, have been first indicated in ref. [12] . Let's explain this fact in more detail. The formula (11) may be presented in the form

$$F_{(0)}^\pi(q^2) = \frac{m^2}{8\Lambda^2}N^2\int_0^1 \exp\left[-\frac{m^2}{2\Lambda^2 x(1-x)}\right]\exp\left[-\frac{q_\perp^2(1-x)^2}{8\Lambda^2 x(1-x)}\right]\cdot \qquad (21)$$

$$\cdot\left[1 - \frac{q_\perp^2(1-x)^2}{4m^2} + \frac{2\Lambda^2}{m^2}x(1-x)\right]\frac{dx}{x(1-x)}$$

In the range $0.1 \lesssim x \lesssim 0.9$ the function $\exp\left[-\frac{m^2}{2\Lambda^2 x(1-x)}\right]$ behaves approximately as $x(1-x)$, therefore, at $q_\perp^2 \lesssim 8\Lambda^2$ the main contribution in the integral comes from the range $(1-x) \lesssim 8\Lambda^2/q_\perp^2$ and in this range we have an approximate power behavior of $F_0^\pi \sim \frac{1}{q_\perp^2}$. At the further increase of $q_\perp^2$ the main contribution comes from the range $(1-x) \sim 1/q_\perp$ and the power behavior transforms gradually to the exponential behavior of the type $e^{-Aq_\perp}$ and at $q_\perp^2 \sim$ 30 (GeV)^2 the contributions of the diagrams of fig. 1a and fig. 2a become equal. However one should keep in mind that in the range of $q_\perp^2 \gtrsim$ (3+5)(GeV)^2 the contribution of the diagram of fig. 2a comes to depend on the form of the vertex function whose be-

havior near $x \to 1$ is not determined by the meson static characteristic. Below we present some remarks on a possible modification of the vertex functions at $x \to 1$.

1. Static characteristics and behavior of the form factor at $q^2 < 3 \div 5\ (\mathrm{GeV/c})^2$ are not very sensitive to the form of the meson wave function, therefore, in this range the use of the exponential formula (18) (for simplicity) appeared possible. In the range $x \to 1$ there is no basis to expect an exponential fall off the wave function, since the effective potential should be Coulombian at small distances.

Hence at $x \to 1$ the wave function should be broader. A simple analysis shows that one always may so modify the wave function as to improve the description of the electromagnetic form factor at $q^2 \gtrsim 5\ (\mathrm{GeV/c})^2$ without violating the description of the static characteristics. For example, replacing $\exp\left[-\frac{m^2}{4\Lambda^2 x(1-x)}\right] \to \sqrt{x(1-x)}$ in the formula (18) with an appropriate coefficient, we obtain the power behavior $\sim 1/q^2$ of the form factor (21) at $q^2 \to \infty$ (the dashed-dot curve in fig. 4).

One should however remember that the contribution of the diagrams without gluon exchanges (fig. 2) must be suppressed at large q^2 by a Sudakov form factor [5]. In this case of modified vertex function the contribution of the diagram of fig. 2 vanishes asymptotically only due to Sudakov suppression and becomes equal to the contribution of the one-gluon exchange diagrams at asymptotic values of $q^2 \sim 10^3(\mathrm{GeV})^2$.

2. The mass of constituent quark m is an effective parameter which should depend on characteristic distances between quarks. At small distances this quantity should decrease (see e.g. [18]), i.e., the effective value of m should decrease with the increase of $q_\perp^2$. As is seen from the formula (21), this effect leads also to the broadening of the distribution $\exp\left[-\frac{m^2}{2\Lambda^2 x(1-x)}\right]$ near $x \to 1$ at large Q^2, and therefore, the range where $F_\pi(Q^2)$ behaves approximately as in this case is also broadened. So keeping in mind the above facts, one can conclude that the value of $Q^2 = Q_0^2 = 20\ (\mathrm{GeV})^2$, when the contributions of diagrams of fig. 1a and fig. 2a became equal, should be considered as a minimum estimate. At $Q^2 > Q_0^2$ the one-gluon exchange mechanism should dominate. However at less values of Q^2 another physical mechanism connected with the overlapping of constituent quark wave functions possibly became involved. Let us assume for estimation the following values of constituent quarks mean-square radius: $\langle r^2 \rangle_q = (0.1 \div 0.05) \langle R^2 \rangle_h \sim (1 \div 0.5)(\mathrm{GeV})^{-2}$ [19]. It is interesting that the small value of quarks a.m.m. $\mu_e = 0.07$ indicates a much smaller value of $\langle r^2 \rangle_q \sim 0.1(\mathrm{GeV})^{-2}$. Thus at $(5 \div 10)(\mathrm{GeV})^2$ the quark clouds forming a constituent quark should overlap and this value of Q^2 should determine the range of validity of our model. At a further increase of one should apparently expect a gradual transition to the quark-parton picture based on the color tube model [8]. If it is really the case the range of validity of perturbative QCD asymptotic formulae will be achieved at very large values of $Q^2 \sim 10^3(\mathrm{GeV})^2$ [8].

Thus the existing experimental data on Q^2 at $\lesssim 6\mathrm{GeV}^2$ are in the range of validity of the theory. In this range the

Sudakov suppression, apparently, doesn't exceed 30% and is approximately compensated by the contribution of one-gluon exchange diagrams. So the contribution of the diagram of fig. 2a approximately corresponds to the form factor true behavior.

It should be also noted that the physical picture underlying our discussion, apparently, corresponds to the mechanism considered in refs. [9,10,11].

4. Electromagnetic form factor of ρ- mesons

The electromagnetic current of ρ- mesons has the following form

$$<P',\lambda'|J_\mu|P,\lambda> = -e_\alpha(P')\ell_\alpha(P)(P+P')_\mu F_1 + [e(P')q][e(P)\cdot q]\cdot$$
$$\cdot(P+P')_\mu F_3 + [e_\mu(P')e(P)\cdot q - e_\mu(P)e(P')\cdot q]F_2 \qquad (22)$$

Consider the contribution of one-gluon exchange diagrams of the type of fig. 1a. Since the two-quark system form factor in the leading in $1/Q^2$ asymptotics is suppressed in the case of parallel helicities of quarks composing a meson, it is reasonable to consider only the combinations of the form factors corresponding to the zero helicities of initial and final ρ mesons.

Let us define the helicity amplitude in the Breit frame ($\mu = 0$)

$$G^\rho = <P',0|J_0|P,0> = F_1(q^2)\left(1+\frac{q_\perp^2}{2M_\rho^2}\right) - F_2(q_\perp^2)\frac{q_\perp^2}{2M_\rho^2} + F_3(q_\perp^2)q_\perp^2\left(1+\frac{q_\perp^2}{4M_\rho^2}\right) \qquad (23)$$
$$G^\rho(0) = 1$$

Carrying out calculations similar to the π -meson case we obtain

$$G^\rho_{(1)} = -\frac{32\pi\alpha_s(Q^2)}{9Q^2}\left[\int_0^1 \frac{\varphi_\rho(x)dx}{2x(1-x)}\right]^2 \qquad (24)$$

Note that (24) differs from the resluts of [3] in its sign. The difference in signs of π and ρ -mesons form factors $F^\pi_{(1)}$ and $G^\rho_{(1)}$ is of a simple nature. It is due to the fact that in the one-gluon exchange diagrams the projections of initial and final quark spins are opposite, and convoluting the two-quark system form factor with effective wave functions of π and ρ -mesons which have (as shown in the previous section) a standard SU(6)-spin structure, we obtain different signs for $F^\pi_{(1)}$ and $G^\rho_{(1)}$.

It is also interesting to consider the simplest quark diagram (fig. 2a) contribution, which supposedly dominates at not very large values of Q^2, to the ρ -meson form factors and compare the results with the analogous results of ref. 10 obtained in the framework of QCD dispersion sum rules. These calculations are now coming to end and will be published in a subsequent paper.

In conclusion let us once more note that the meson static characteristics and available data [20] on the π -meson form factor may be consistently described in the framework of a relativistic quark model on the basis of a simple quark diagram of fig. 2a. The contribution of the one-gluon mechanism in the pion form factor doesn't exceed 30% and isn't determining in the experimentally observable power law (1).

We would like to thank I.G.Aznauryan, A.B.Kaidalov, S.G.Matinyan and S.Petkov for discussions.

Table 1. Results of the description of meson low-energy parameters in relativistic quark model. The presented experimental value of $\langle R^2 \rangle$ is a result of averaging the available data.

	experiment	m = 0.20 GeV Λ_π =0.540GeV Λ_ρ =0.420GeV	m =0.26GeV Λ_π=0.415GeV Λ_ρ=0.415GeV	m =0.36GeV Λ_π=0.357GeV Λ_ρ=0.415GeV
f_π (GeV)	$9.3\ 10^{-2}$	$8.93\ 10^{-2}$	$9.27\ 10^{-2}$	$9.29\ 10^{-2}$
$M_\rho f_\rho$ (GeV)^2	$1.19\ 10^{-1}$	$1.19\ 10^{-1}$	$1.18\ 10^{-1}$	$1.13\ 10^{-1}$
$f_{\omega\pi}$ (GeV^{-1})	0.785 ± 0.025	0.690	0.757	0.672
$\langle R^2 \rangle$ (GeV^{-2})	14.4 ± 5.4	11.0	12.4	11.4

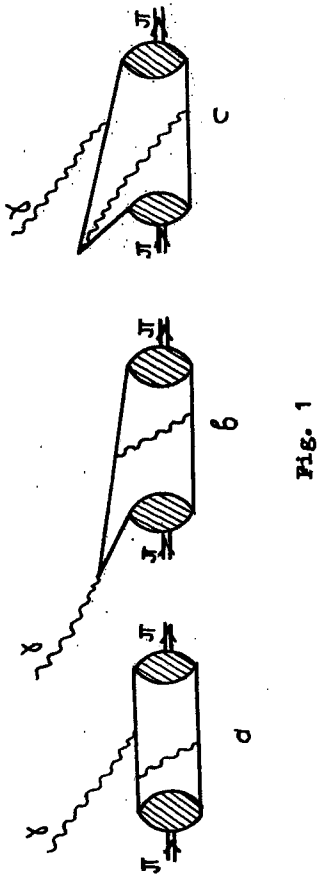

Fig. 1

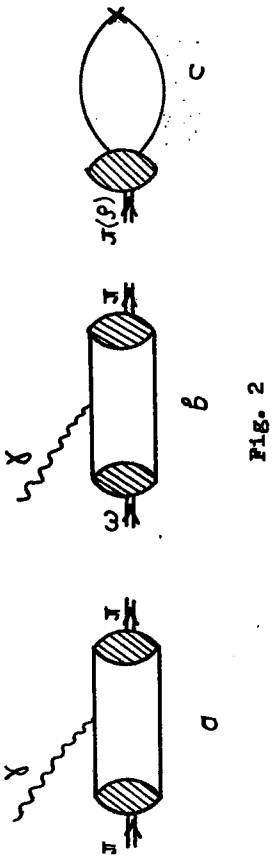

Fig. 2

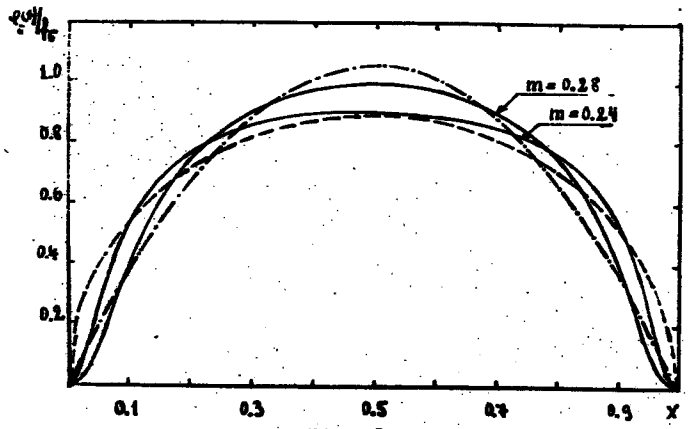

Fig. 3

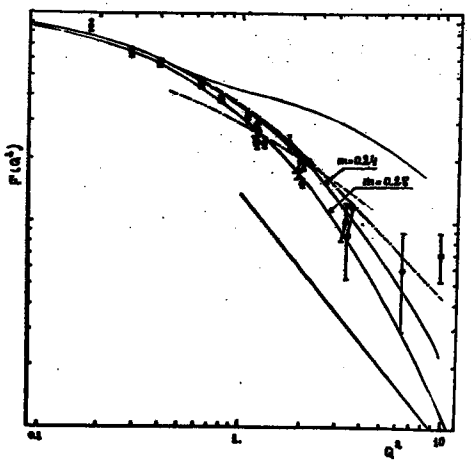

Fig. 4

Figure Captions

Fig. 1 Diagrams of old fashioned perturbation theory determining the asymptotics of the meson electromagnetic form factors.

Fig. 2 a) Diagram determining the behavior of electromagnetic form factor at moderate Q^2.

b) Diagram corresponding to $\omega(\rho) \to \pi\gamma$ decay.

c) Diagram corresponding to constants f_π and f_ρ. The cross denotes the axial (vector) current.

Fig. 3 Meson wave functions (13) for the two values of parameters: m = 0.28 GeV, Λ = 0.39 GeV and m = 0.24 GeV, Λ = 0.442 GeV. For comparison the asymptotical wave function (dashed-dot curve) and the wave function of the type $\varphi(x) = \frac{4f_\pi}{\pi}\sqrt{2x(1-x)}$ (dashed curve) are presented.

Fig. 4 Pion electromagnetic form factor in a relativistic quark model. The lower straight line corresponds to the one-gluon exchange contribution. The upper curve corresponds to the wave function of ref.[7]. Curves m =0.24 GeV and m =0.28 GeV correspond to the contribution of the fig. 2a diagram for the values Λ =0.442 GeV and Λ =0.39 GeV, respectively. The dashed-dot curve corresponds to the modified wave function. Results of ref. [9] (dashed curve) are presented for comparison.

References

1. Matveev V.A., Muradyan R.M., Tavkhelidze A.N. Automodelism in the Large-Angle Elastic Scattering and Structure of Hadrons.- Nuovo Cim.Lett., 1973, vol.7, p.719-723.
2. Brodsky S.J., Farrer G.R. Scaling Laws for Large-Momentum Transfer Processes.- Phys.Rev. D, 1975, vol.11, No.5, p.1305-1330.
3. Черняк В.Л. Асимптотическое поведение эксклюзивных амплитуд в квантовой хромодинамике. Материалы XУ Зимней школы ЛИЯФ, Ленинград, I980, с.65-I54.
4. Aznauryan I.G., Esaybegyan S.V., Ter-Isaakian N.L. On the Asymptotics of the Nucleon Form Factors in the Quark-Gluon Model.- Phys.Lett., 1980, vol. 90b, p.151-154.
5. Brodsky S.J., Lepage G.B. Perturbative Quantum Chromodynamics. SLAC-PUB-2447, 1979, p.1-168.
6. Ефремов А.В,Радюшкин А.В. Асимптотика формфактора пиона в квантовой хромодинамике,ТМФ, I980, т 42,№2 с.I47-I66
7. Chernyak V.L., Zhitnitsky A.R. On the Calculation of the Meson Wave Function.- Institute of Nuclear Physics, Novosibirsk preprint 81-74.
8. Kaidalov A.B. Electromagnetic Form-Factors of Hadrons at Large Q^2 and Effects of Confinement. ITEP-79, Moscow 1980
9. Ioffe B.L., Smilga A.V. Pion Form-Factor at Intermediate Momentum Transfer in QCD. Preprint ITEP-27, Moscow 1982.
10. Ioffe B.L., Smilga A.V. Meson Widths and Formfactors at Intermediate Momentum Transfer in Nonperturbative QCD. reprint ITEP-100, Moscow 1982.

11. Nesterenko V.A., Radyushkin A.V. Sum Rules and Pion Form Factor in QCD. Preprint JINR-E2-82-204, 1982.
12. Терентьев М.В. О структуре волновых функций мезонов как связанных состояний релятивистских кварков, НФ, т 24 I976, с.207-2I3
13. Берестецкий В.Б.,Терентьев М.В. Динамика светового фронта и нуклоны из релятивистских кварков, НФт24, I976, с.IC44-IC57
14. Терентьев М.В. Мезоны из релятивистских кварков. Препринт ИТЭФ-6, Москва, I976.
15. Aznaurian I.G., Bagdasarian A.S., Ter-Isaakian N.L. Relativistic Quark Model in Infinite Momentum Frame and Static Properties of Hadrons. EPI-550(37)-82, p.1-37.
16. Melosh H.J. Quarks Currents and Constituents.- Phys.Rev., 1974, vol. D16, p.1095-1112.
17. Азнаурян И.Г.,Тер-Исаакян Н.Л.Аномальные магнитные моменты кварков в магнитно-дипольных переходах адронов, НФ 3I, I980, вып.6, с.I680-I689
18. Politzer H.D. Effective Quark Masses in the Chiral Limit.- Nucl.Phys., 1976, vol. B117, No.2, p.397-406.
19. Анисович В.В.. Составляющие кварки и партоны в мягких процессах. Материалы XIУ Зимней школы, ЛИЯФ,Ленинград,I979.
20. Mobsh C.J., Brown C.N., Holmes S.D. et al. Electroproduction of Single Pions at Low ε and the Measurement of the Pion Form Factor up to Q^2= 10 GeV^2.- Phys.Rev. D, 1978, vol. 17, No.7, p.1693-1705.

The manuscript was received 26 July 1982.

А.С.БАГДАСАРЯН, С.В.ЕСАЙБЕКЯН, Н.Л.ТЕР-ИСААКЯН

РЕЛЯТИВИСТСКАЯ МОДЕЛЬ КВАРКОВ И ПОВЕДЕНИЕ ЭЛЕКТРОМАГНИТНЫХ ФОРМФАКТОРОВ МЕЗОНОВ В ОБЛАСТИ МАЛЫХ И ПРОМЕЖУТОЧНЫХ Q^2

(на английском языке, перевод Л.Н.Багдасаряна)

Ереванский физический институт

Редактор Л.П.Мукаян

Тех.редактор А.С.Абрамян

Заказ 590 ВФ- 04029 Тираж 299

Препринт ЕФИ Формат издания 60x84/16

Подписано к печати 8/XII-82 I,5 уч.-изд.л.Ц.22 к.

Издано Отделом научно-технической информации

Ереванского физического института, Ереван 36, Маркаряна 2